J Therm Anal Calorim (2012) 108:323–332
DOI 10.1007/s10973-011-1954-2

Physicochemical characterization of nicergoline and cabergoline in its amorphous state

Valentina Martena · Roberta Censi · Ela Hoti · Ledjan Malaj · Piera Di Martino

Received: 31 May 2011 / Accepted: 21 September 2011 / Published online: 11 October 2011

Abstract Formulation of poorly water-soluble crystalline drugs into their more soluble amorphous form is a common approach for improving their bioavailability. In this study, the amorphous forms of nicergoline (NIC) and cabergoline (CAB) were obtained by different methods (melting and precipitation under solvent evaporation). The physicochemical characteristics of the samples were determined by HPLC, differential scanning calorimetry (DSC), thermogravimetry, and X-ray powder diffractometry. The physical stability of the amorphous forms was investigated by DSC by considering how the onset temperature and the enthalpy content at the glass transition vary with aging time and temperature. Using the Kohlrausch–Williams–Watts equation on the data obtained from the experiments, the "mean molecular relaxation time constant" (τ) was estimated. This parameter was used to understand the stability of NIC and CAB in their glassy state at different temperatures, and results showed that their stability is adequate to enable the formulation of these drugs into solid dosage forms.

Keywords Nicergoline · Cabergoline · Amorphous · Thermal analysis · Mean relaxation time constant

V. Martena · R. Censi · L. Malaj · P. D. Martino (✉)
School of Pharmacy, University of Camerino, Via S. Agostino 1, 62032 Camerino, Italy
e-mail: piera.dimartino@unicam.it

E. Hoti · L. Malaj
Department of Pharmacy, University of Tirana, Street of Dibres, Tirana, Albania

Introduction

Amorphous drugs may prove important for pharmaceutical formulations because their greater apparent solubility and faster dissolution rates may lead to higher bioavailability [1]. Since, the majority of drugs in crystalline form are poorly water soluble, the potential to transform them into an amorphous state is regarded with interest because of the advantageous biopharmaceutical properties that might thus be obtained. An amorphous phase may be deliberately formed to improve the dissolution rate and bioavailability of poorly soluble compounds [2]. Amorphous systems, indeed, by virtue of their disordered nature possess appreciably lower packing energy than crystalline forms, where crystal packing energy is referred to as the energy required to disrupt the crystal packing and allow participation of the solute in dissolution [3].

The major limitation in the use of amorphous pharmaceutical forms is the tendency to devitrification, due to their high thermodynamic instability. Several attempts have been made to enhance the physicochemical and thermodynamic stability of amorphous forms by combining the amorphous pharmaceutical ingredient with an appropriate excipient into solid dispersions [4–8].

Information on the physicochemical stability of the amorphous form of a pure drug could prove invaluable in predicting its potential for use in medicinal formulations.

This study focused on two active pharmaceutical ingredients, the semisynthetic ergot derivatives nicergoline (NIC) and cabergoline (CAB), which are water insoluble in their crystalline states.

NIC (10α-methoxy-1,6-dimethylergoline-8β-methanol-5′-bromonicotinate) ($C_{24}H_{26}BrN_3O_3$) is a potent blocking agent for α_1-adrenoreceptors [9] and shows remarkable effects in lowering systemic blood pressure and dilating

blood vessels [10]. NIC has also been clinically used for the treatment of senile dementia [11], for its cerebral-anti-ischemic action [12, 13], and in the early phases of acute myocardial infarction, because it lowers myocardial oxygen consumption [14]. NIC exists in two different polymorphic forms [15–18].

CAB (*N*-[3-(dimethylamino)propyl]-*N*-(ethylcarbamoyl)-6-allyl-ergoline-8β-carboxamide) exhibits a long-term agonistic activity on the D_2 dopamine receptor. Due to its potent and very long acting inhibition of prolactin secretion, it is used for the treatment of hyperprolactinemia and Parkinsonism [19, 20]. CAB exists in different polymorphic forms and solvates [21–23].

The objective of this study is the characterization of the physicochemical properties of NIC and CAB in their amorphous state, the existence of which is demonstrated in this study for the first time. In this study, the amorphous forms of NIC and CAB were obtained by different methods:

a. an in situ preparation method, supercooling the melt in the differential scanning calorimeter (DSC);
b. melting and subsequent supercooling of the melt obtained in an oven;
c. dissolution of the drugs in chloroform and recovering the amorphous form after solvent evaporation under reduced pressure.

Experimental

NIC and CAB were purchased from China-Japan Shandong Hongfuda Pharmchem Co., Ltd. (Shandong, China) as white crystalline powders. For the experiments of this study, both powders were used as received.

The molecular structures of the drugs are given in Fig. 1, and the empirical formula and molecular weight of both drugs are indicated in Table 1.

Amorphous forms of NIC and CAB were obtained by three different methods:

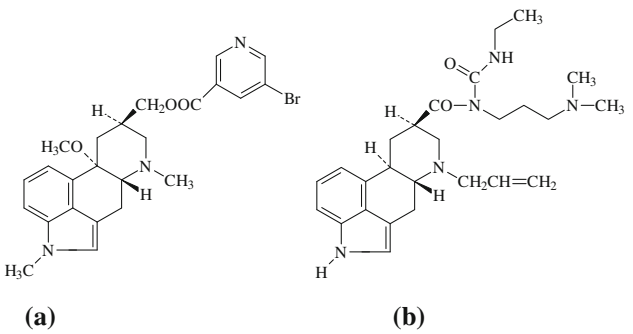

Fig. 1 Chemical structure of NIC (**a**) and CAB (**b**)

Table 1 Summary of some important physicochemical and thermodynamic parameters of NIC and CAB in their solid state (crystalline and amorphous)

	NIC	CAB
Empirical formula	$C_{24}H_{26}BrN_3O_3$	$C_{26}H_{37}N_5O_2$
Molecular weight/dalton	484.44	451.60
Melting temperature T_m/K	408.11 ± 0.48	369.84 ± 0.53
Enthalpy of melting ΔH/J g^{-1}	58.23 ± 1.26	60.66 ± 1.33
Glass transition temperature[a] T_g/K (onset)	322.21 ± 0.83	324.42 ± 0.78
Change in specific heat at T_g ΔC_p/J g^{-1} K	0.204	0.256
T_m/T_g	1.267	1.140
Specific heat crystalline C_{pc}/J g^{-1} K[b]	1.162	1.258
Specific heat liquid C_{pl}/J g^{-1} K[b]	1.376	1.531
Kauzmann temperature T_K/K[c]	122.67	132.89
Kauzmann temperature T_K/K[d]	136.01	147.64

[a] Determined without aging in DSC apparatus (*Method A*)

[b] Determined by SS-DSC

[c] Calculated according to Eq. 4

[d] Calculated according to Eq. 5

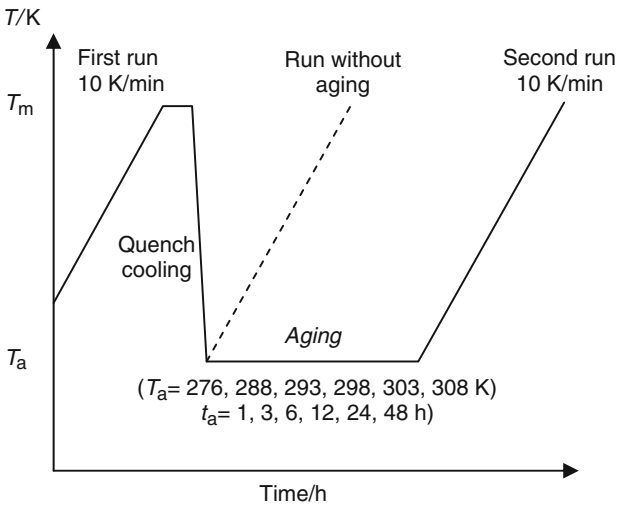

Fig. 2 Schematic representation of the thermal procedure applied in the DSC during the aging experiments

(1) Drugs were melted in the DSC, according to the thermal procedure described in Fig. 2. This procedure will be referred to as *Method A*, and is fully described in the paragraph "Differential Scanning Calorimetry analysis". This method was only applied to the evaluation of the drug stability.
(2) Drugs were melted in a ventilated oven: crystalline drug is placed in closed vials in the presence of nitrogen gas, melted at the melting temperature and cooled by spontaneous cooling to room temperature;

the amorphous solid was then ground in a mortar. This procedure will be referred to as *Method B*.

(3) Drugs were dissolved in chloroform (Sigma-Aldrich, Steinheim, Germany) and solvent was evaporated under reduced pressure at 25 °C. The residual solvent was removed under vacuum in the presence of liquid nitrogen. The viscous amorphous NIC was stored for approximately 24 h at a temperature lower than the glass transition temperature to obtain a solid amorphous form, which was then ground for further purposes. This procedure was referred to as *Method C*.

All the amorphous products obtained by the different procedures were stored in tightly closed vials placed in a desiccator in the presence of P_2O_5 as desiccant preventing the contact with the humidity that may influence the stability of the amorphous drugs. Other chemicals were: methanol, formic acid (HCOOH), triethanolamine (Et_3N), and acetonitrile (Sigma-Aldrich, Steinheim, Germany). Ultrapure water was produced by Gradient Milli-Q® (Millipore, Molsheim, France).

HPLC analysis was performed by a HPLC 1100 (Agilent Technologies, Santa Clara, CA, USA) equipped with a detector VWD 1200 (Agilent Technologies). Separation was performed on a reversed-phase column (Purospher C_{18} 4.6 × 125 mm i.d., 5 µm, Merck, Milan, Italy) using a mobile phase consisting of a mixture of A + B in the ratio 40:60 [A = water + triethanolamine (0.2% VV) + formic acid (15 mM) pH = 6.3; B = acetonitrile]. The detection wavelength was 290 nm. Samples (2 µL) were injected manually at the concentration of 3.0 mg/mL in methanol. The flow rate was 1 mL/min.

Thermogravimetric (TG) analysis was carried out by the simultaneous thermal analysis (STA) which enables to simultaneously analyse a sample for change in mass (TG analysis) and change in enthalpy flow (differential scanning calorimetry, DSC). In this text, TG analysis is abbreviated as STA-TG. The analysis was performed with a simultaneous thermal analyser (STA 6000, Perkin Elmer, Inc., Waltham, MA, USA), under nitrogen atmosphere (flow rate of 20 mL/min) in 0.07 mL open aluminum oxide pans. STA was calibrated for temperature and heat flow with three standard metals (tin, indium, and zinc), taking into account their expected melting temperatures (505.08, 429.75, and 692.68 K, respectively), and for mass with an external Perkin Elmer standard (Calibration Reference Weight P/N N520-0042, Material lot 91101 GB, Weight 55.98 mg, 01/23/08 VT). Calibration was repeatedly checked to assure deviation $\leq \pm 0.3$ K. This method was used to assess the total mass loss of samples. Analyses were preformed from 288 to 20 K over the drug melting at 10 K min^{-1}.

Differential scanning calorimetry (DSC) analysis was performed on a Pyris 1 (Perkin Elmer, Co. Norwalk, USA) equipped with a cooling device (Intracooler 2P, Cooling Accessory, Perkin Elmer, Co. Norwalk, USA). A dry purge of nitrogen gas (20 mL/min) was used for all runs. DSC was calibrated for temperature and heat flow using a pure sample of indium and zinc standards. Sample mass was about 4–5 mg and aluminum perforated pans of 50 µL were used. Particular precautions were taken to minimize the interfering effect of sample mass, thermal contact, and heat transfer lags.

The amorphous glassy forms were prepared in DSC by quench cooling of the melt (*Method A*) according to the thermal procedure described in Fig. 2. Drugs were heated at 10 K min^{-1} to a temperature 5 K above the melting temperature, and kept isothermal for 5 min to assure complete melting of the drug. The melt was quench cooled at approximately 200 K min^{-1} cooling rate to different aging temperatures (T_a) (276, 288, 293, 298, 303, and 308 K). Samples were maintained at the aging temperature for a predetermined period of aging time (t_a) (1, 3, 6, 12, 24, and 48 h). Subsequently, after different t_a, the glassy materials were heated at 10 K min^{-1} up to the expected melting temperature. This second heating run was used to determine the extrapolated onset glass transition temperature (T_g), the enthalpy recovery (ΔH), and the change in heat capacity (ΔC_p). The parameters associated with the glass transition temperature and determined by this procedure are given in Fig. 3. A cycle for an un-aged sample was also run, and in this case, after the melting and cooling steps, a second heating run was carried out immediately without any isothermal aging step. Because, the T_g is highly dependent upon the conditions under which glass was formed (cooling conditions) [24] and upon T_g measurement conditions (heating conditions) [25], particular

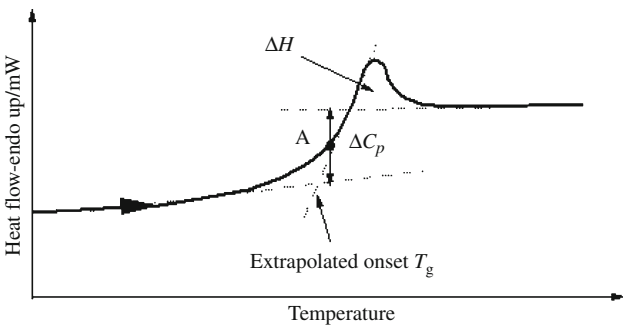

Fig. 3 Depiction of the parameters associated with the glass transition (T_g) and calculated for the evaluation of the mean relaxation time constant (τ). *A* represents the mean value between the two baselines indicated by *dotted lines*. Difference between these two lines makes it possible to evaluate change in specific heat (ΔC_p). ΔH represents the relaxation enthalpy associated with aging treatments

care was taken to standardize the entire procedure. The values used for each parameter were the mean values determined from four replicated samples. The entire procedure is schematically depicted in Fig. 2.

The heat capacities at constant pressure (C_p), the reversing and non-reversing signals were measured by DSC using the Step Scan® software of Perkin Elmer for the crystalline and liquid phases of each drug (the technique will be henceforth referred to as SS-DSC). This technique has been frequently used to determine the C_p [26, 27]. The heat capacities were obtained by deconvolution of the total heat flow curve into the reversing and the non-reversing phenomena. Heat capacities were measured for the drugs in their crystalline phase over a temperature range from 273 to 10 K above the melting temperature.

In the case of the liquid phases, the range was between 273 and 343 K. The SS-DSC heating scans were obtained at an average rate of 2 K min^{-1} with a period of 60 s (temperature increment of 2 K with each 30 s isothermal and scanning segments). Data for isothermal segments were collected within the 0.005 mW s^{-1} criteria. Specific heat calculation for heat flow response was carried out using the area under each segment of the curve. For each scan, a baseline was recorded with matched empty aluminum pans using the same method. All SS-DSC curves were corrected using the appropriate baselines recorded under identical conditions and converted to specific heat capacity curves.

X-ray powder diffractometry (XRPD) was used to check the amorphous state of the studied samples and to evaluate their physical stability. For this purpose, a Philips PW 1730 (Philips Electronic Instruments Corp., Mahwah, NJ, USA) as X-ray generator for Cu Kα radiation ($\lambda_{\alpha 1} = 1.54056$ Å, $\lambda_{\alpha 2} = 1.54430$ Å) was used. The experimental X-ray powder patterns were recorded on a Philips PH 8203. The goniometer supply was a Philips PW 1373 and the channel control was a Philips PW 1390. Data were collected in the discontinuous scan mode using a step size of 0.01° 2θ. The scanned range was from 2° to 40° (2θ).

Results

Physicochemical characterization of NIC and CAB amorphous forms

X-ray powder diffraction patterns of native NIC and CAB show well-defined peaks, typical of crystalline structures. The diffractograms of the NIC and CAB obtained by the Method C is typical of amorphous forms. Diffractograms of NIC and CAB obtained by Method B are identical to those obtained by Method C, but they are not reported for simplicity (Fig. 4).

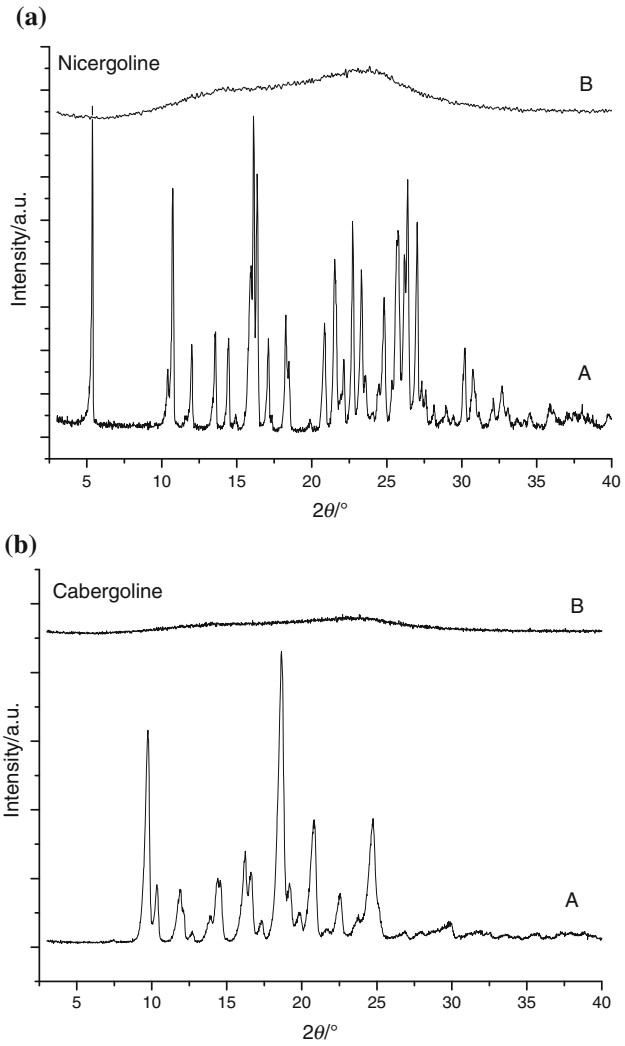

Fig. 4 XRPD of crystalline (native) (*A*) and amorphous forms (*B*) of NIC (**a**) and CAB (**b**)

Table 2 Mass loss/% of NIC and CAB obtained by different preparation methods and determined by TG

	Mass loss/%[a]
NIC	
Native	0.112 ± 0.015
Amorphous method A	0.085 ± 0.020
Amorphous method B	0.092 ± 0.012
Amorphous method C	0.087 ± 0.023
CAB	
Native	1.248 ± 0.014
Amorphous method A	1.361 ± 0.027
Amorphous method B	1.352 ± 0.022
Amorphous method C	1.228 ± 0.030

[a] Determined by TG from 293 K to drug melting temperature

TG analyses of NIC and CAB showed that regardless of the preparation method there was no significant mass loss for amorphous NIC and CAB as compared to their native crystalline form. Results are indicated in Table 2. In general, amorphous solids have high hygroscopicity and tend to absorb humidity not only on the surface, but also into their internal structure once exposed to different relative humidities % [28, 29]. In addition, it was demonstrated that water acts as a plasticizer and was thus identified as the main cause for amorphous solids crystallization. Water, indeed, decreases the glass transition temperature, improving molecule mobility (at temperatures near room temperature) and leading to crystallization of amorphous solids [30, 31]. To exclude the influence of water on the re-crystallization process of NIC and CAB, each amorphous sample was stored in dry conditions, as described in "Materials and methods". Therefore, the objective of this study was to evaluate the stability of NIC and CAB independently of the influence of humidity.

By TG, it was also possible to determine that no mass loss was associated with the melting endotherm, confirming that during melting and in the presence of nitrogen gas no chemical degradation occurred for both drugs. These results demonstrated that for all the used preparation methods (A, B, and C) the chemical stability of NIC and CAB was maintained in their amorphous forms. This finding was further confirmed by HPLC. Figure 5 shows the chromatograms of NIC and CAB, and for each drug one peak was detected, the retention times of which were 0.653 and 1.861 min, for NIC and CAB, respectively. HPLC chromatograms of amorphous NIC and CAB comply with those of crystalline native drugs, confirming that no degradation occurred during drug handling.

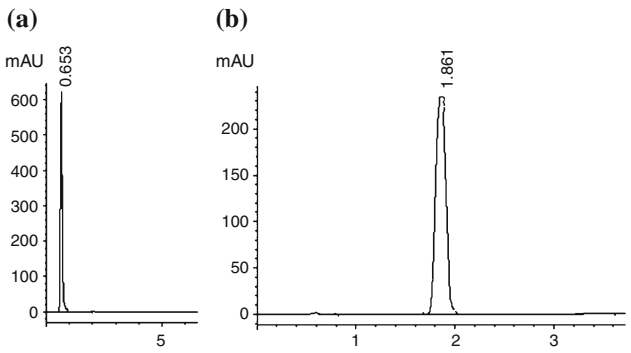

Fig. 5 HPLC chromatograms of NIC (**a**) and CAB (**b**). The chromatograms reported correspond to the solutions prepared from native drugs. Chromatograms of solutions prepared from drugs obtained from methods A, B, and C are identical, thus not reported here

DSC analysis and evaluation of physicochemical stability of NIC and CAB amorphous forms

This study was based on the assumption that the average rate of molecular motions at any given temperature is one the most important parameter for amorphous pharmaceutical materials, as it can be used to predict the stability of drugs at different temperatures [32, 33]. The reduced stability of amorphous solids is due to their greater molecular mobility as compared to their crystalline form [34]. Consequently, information on the relationship between molecular mobility and storage conditions is of considerable importance, and molecular mobility can be used to understand the stability of the same system at different temperatures.

Differential Scanning Calorimetry is frequently used by pharmaceutical scientists because of its convenience, time effectiveness, and small sample requirements, and because it can be effectively used at temperatures below the T_g. In this study, DSC was a valuable tool in predicting the physicochemical stability of NIC and CAB in their amorphous state in accelerated conditions, based on the evaluation of the "mean relaxation time constant" τ [35–38].

According to the experimental procedure outlined in Fig. 2, NIC and CAB were melted in the DSC apparatus (*Method A*). The curve of the first heating run (given in Fig. 6 for both NIC and CAB) shows the corresponding melting endotherms. The melting temperatures (T_m) and the associated enthalpy changes (ΔH) are indicated in Table 1. A significant difference in T_m between the two drugs may be pointed out, in spite of the great chemical similarity of the two structures. During the temperature scan, no decomposition occurs (generally revealed by endothermic or exothermic events associated or not with the melting peak). This evidence, associated to the results obtained by TG and HPLC, permitted to conclude about the stability of NIC and CAB in the thermal interval considered for this study. A second heating run, carried out for both drugs immediately after quench cooling and thus without aging, is also given in Fig. 6. The curves show the glass transitions, and the corresponding parameters associated with the T_g are indicated in Table 1. The T_gs of the two drugs are very similar, while significant differences in their ΔC_p may be noted. It is interesting to observe that no crystallization occurs during heating and consequently there is no melting peak for both drugs. This phenomenon was observed also during the aging experiments: no crystallization occurred at any aging temperature and time.

The DSC analyses of NIC and CAB obtained by methods B and C showed curves similar to those obtained during the second heating: the curves showed the glass transition but no crystallization and melting peaks were observed. For NIC, the T_g was 325.16 ± 1.44 and 327.48 ± 1.12, for *Methods B* and *C*, respectively. For CAB, the T_g was 327.22 ± 1.38 and 328.56 ± 1.85, for *Methods B* and *C*, respectively. Differences in T_g according to the preparation method may be explained by the fact that the glass transition temperature is

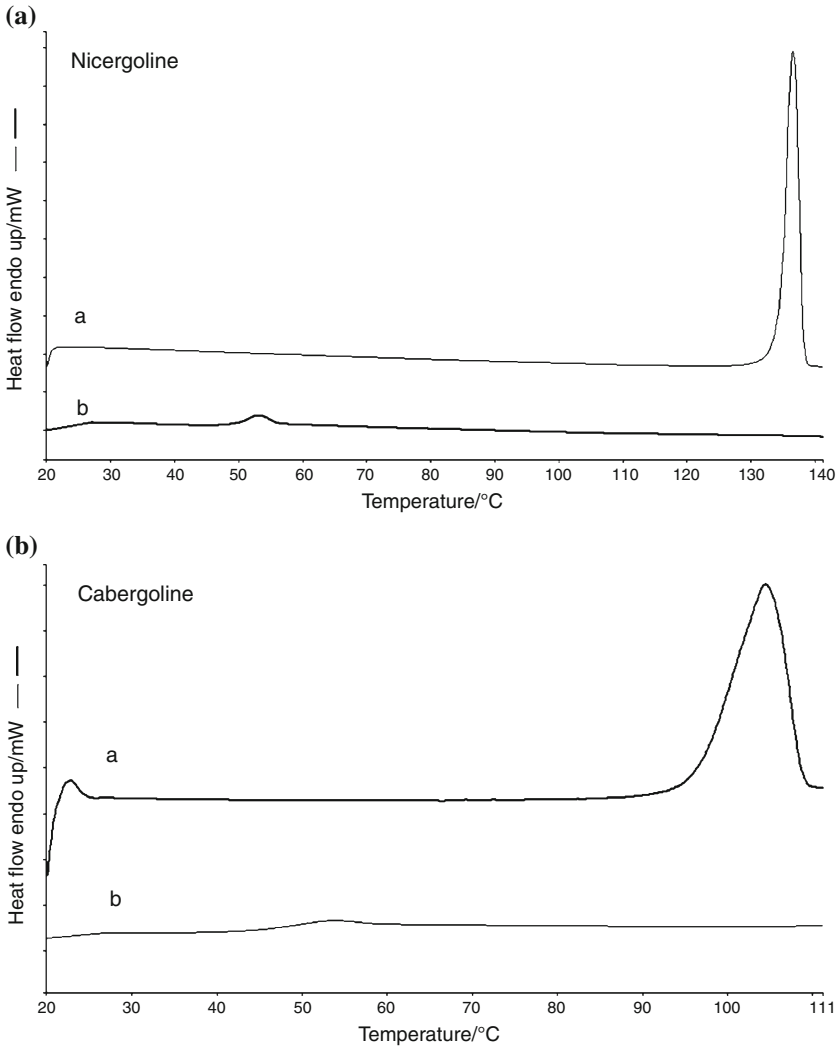

Fig. 6 DSC curves of NIC and CAB corresponding to the first heating run of the crystalline drugs (*a*) and second heating run (*b*) immediately after quench cooling (without aging)

strongly influenced by the preparation conditions of the glassy material (for example, the cooling conditions, the presence of residual solvents, etc.) [39].

Since, the physical instability of amorphous forms is ascribable to their high molecular mobility, thus high crystallization tendency, the lack of crystallization of amorphous forms during heating cycles may be considered as a first macroscopic and empirical sign of their relative stability. Therefore, it can be concluded that amorphous forms of NIC and CAB display a relatively stable nature. The stability of the amorphous forms of other drugs has been reported in several studies. For example, Chawla and Bansal [3] described similar observations and affirmed the stability of the amorphous form of irbesartan. Conversely, Di Martino et al. [25] observed the low stability of the paracetamol amorphous form and reported that its crystallization after melting and quench cooling always occurred independently of the aging time and temperature. They showed that aging conditions influence the polymorphic form obtained under crystallization and that the more stable form I was favoured when the structural equilibrium was reached during the experimental time interval. Crystallization of indomethacin and phenobarbital occurred even at temperatures below their T_g, indicating the high molecular mobility of these drugs in their amorphous state [30, 40, 41]. By DSC, Gashi et al. [8] observed the crystallization of fenbufen and naproxen even during the cooling subsequent to drug melting, and reported that their attempts to prevent crystallization during cooling were unsuccessful. They concluded that these two drugs have high instability in the amorphous state, and, in particular, that fenbufen and naproxen liquid phases tend to efficaciously transfer the free energy derived from melting, thus favouring crystallization and consequent stabilization of the system to the minimum energy level. The significance of this behavior was found on the intense molecular movement that occurs, favouring free energy loss and crystallization that is the establishment of intermolecular bonds.

DSC can be used to measure the stability of a solid in its amorphous state (by means of the molecular mobility) because the aged material shows an endothermic relaxation

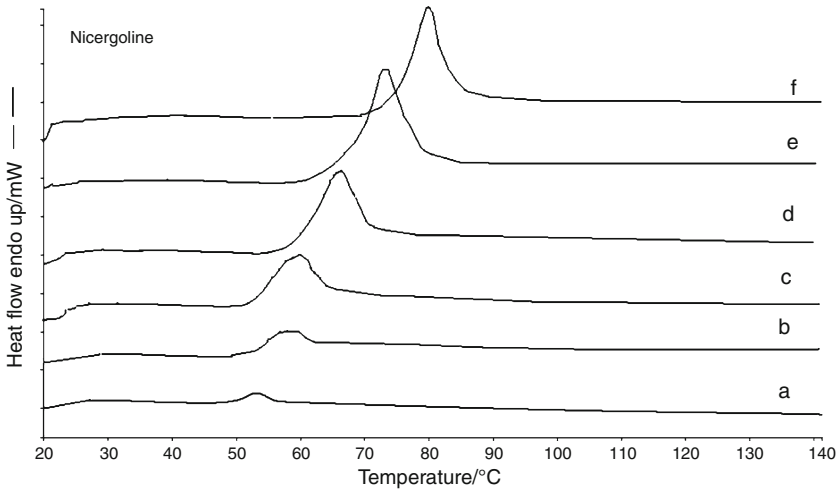

Fig. 7 DSC curves of NIC at an aging temperature (T_a) of 298 K at different aging times (t_a). *a* 1 h; *b* 3 h; *c* 6 h; *d* 12; *e* 24 h; *f* 48 h

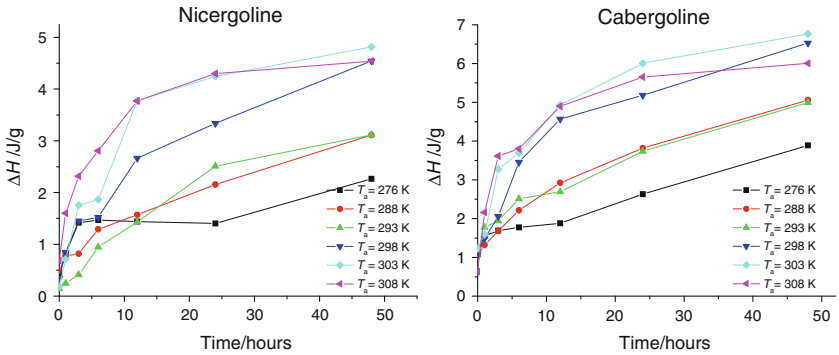

Fig. 8 Evolution of the relaxation enthalpy (ΔH_t) associated with the glass transition temperature (T_g) with time for NIC and CAB for any t_a and T_a

peak corresponding to its glass transition temperature (Fig. 3) [42]. The intensity of this peak depends upon the aging conditions, in particular time and temperature, and the behavior at any given experimental conditions is typical of any solid. Figure 7 provides an example of the DSC curve showing the endothermic relaxation peak associated with the T_g of NIC at different aging times (1, 3, 6, 12, 24, and 48 h) and at a T_a of 298 K. One can note the progressive enthalpy increase associated with the relaxation peak of the T_g and the displacement of the onset glass transition temperature to higher values with aging time. The intensity of these peaks corresponds to the enthalpy content (the relaxation enthalpy, ΔH_t) and can be plotted versus aging time showing the evolution of the relaxation process at any given time and temperature for NIC and CAB (Fig. 8). The relaxation enthalpies increase with aging time for both drugs at any aging temperature; the lowest relaxation enthalpy was found for the lowest aging temperatures considered for this study ($T_a = 276$ K). At the aging temperatures nearest to T_g (298, 303, and 308 K) there is a remarkable increase in ΔH_t within the first 20 h of aging, after which ΔH_t tends to reach a plateau value. This plateau value was reached only during the experiments at 308 K, meaning that equilibrium is actually reached at this temperature during the time scale of the experiments. At lower aging temperatures, the time needed to reach the maximum relaxation enthalpy will be very long and consequently the stability of the glassy amorphous form will increase.

To determine the average relaxation time from the enthalpy change versus storage time data, it is necessary to know the extent to which the glass has relaxed at any time. This requires estimation of the maximum possible enthalpy recovery (ΔH_∞) at any aging temperature (T_a) using Eq. 1:

$$\Delta H_\infty = \Delta C_p \times \left(T_g - T_a\right), \quad (1)$$

where ΔC_p is the heat capacity change at T_g and T_a is the aging temperature. According to Bauwens-Crowet and Bauwens [43] and Kemish and Hay [44], ΔC_p is assumed to be constant and temperature independent. In this study, ΔC_p was calculated as averaged value of six different results (Table 1).

The extent to which a glassy material relaxes (ϕ_t) under any given conditions of time (t) and temperature (T) was determined from Eq. 2:

$$\phi_t = 1 - \left(\frac{\Delta H_t}{\Delta H_\infty}\right), \quad (2)$$

where ΔH_t is the measured relaxation enthalpy under those conditions and ΔH_∞ is the maximum enthalpy recovery calculated from Eq. 1.

The physical stability prediction of the amorphous form was based on the estimation of the "mean molecular relaxation time constant" (τ) and done by fitting the relaxation function to a two-parameter function according to the Kohlrausch–Williams–Watts (KWW) equation (Eq. 3) [45]:

$$\phi_t = 1 - \frac{\Delta H_t}{\Delta H_\infty} = \exp\left(-\left(\frac{t}{\tau}\right)\right)^{\beta}. \quad (3)$$

This function describes non-symmetrical relaxation behavior, and it is frequently applied to quantify the structural relaxation process in glassy materials. Any measured value for τ should be regarded as an instantaneous measure of molecular mobility for the sample and not an equilibrium value. For pharmaceutical systems, one may desire a strong or a weak dependence of τ on temperature, according to the application and circumstances at hand. β is a relaxation time distribution parameter ranging from 0 to 1. If β is equal to unity, there is a single relaxation time and data can be described using a single relaxation time model. In general, the β value varies according to the chemical structure of the molecule involved, but it is generally reported to have only slight variations with temperature [42]. Values of β parameters are similar at different aging temperatures and significantly different from unit, which indicates a distribution of time scales rather than one single relaxation time.

Table 3 summarizes the τ and β values obtained for NIC and CAB at any T_a. The β values are consistent for all the aging temperatures and significantly different from 1, which indicates a distribution rather than one single relaxation time. The β value is always 0.333 for NIC, while it ranges between 0.200 and 0.333 for CAB.

Table 3 Parameters relative to the KWW equation expressed as a function of the aging temperature (T_a) for NIC and CAB

	T_a/K	β	R	τ/h
Pure NIC	276	0.333 (±0.010)	−0.991	12330.000 (±51.312)
	288	0.333 (±0.022)	−0.951	1223.990 (±18.113)
	293	0.333 (±0.013)	−0.986	606.061 (±7.882)
	298	0.333 (±0.032)	−0.992	104.275 (±2.315)
	303	0.333 (±0.016)	−0.963	93.196 (±0.688)
	308	0.333 (±0.024)	−0.992	5.450 (±0.121)
Pure CAB	276	0.200 (±0.032)	−0.985	32658.390 (±128.801)
	288	0.200 (±0.021)	−0.950	1849.283 (±23.011)
	293	0.333 (±0.042)	−0.992	917.432 (±3.127)
	298	0.333 (±0.037)	−0.961	62.112 (±1.223)
	303	0.333 (±0.018)	−0.994	58.858 (±1.668)
	308	0.333 (±0.022)	−0.995	16.137 (±0.125)

The mean relaxation time constants (τ) decreased with increasing aging temperature in both systems studied. Close to T_g (T_a of 308 K), the mean relaxation time constant (τ) is very small and similar for both products (5.450 and 16.137 h, respectively, for NIC and CAB), indicating very low stability of the amorphous forms at this aging temperature. As the aging temperature decreases, τ becomes larger. The difference in τ between the two molecules is always of the same order of magnitude. Very interestingly, at the lowest T_a used for the experiments of this study (276 K), the τ drastically increases for both drugs: 12330 h for NIC and 32658 h for CAB. This means that the stability of NIC and CAB is very high at this aging temperature and thus quite suitable for industrial purposes.

To further evaluate the stability of the amorphous form of these two drugs, the calculation of the Kauzmann temperature (T_K) may be useful. The T_K is the temperature at which the thermodynamic properties (entropy, enthalpy) of the crystalline and the supercooled liquid states converge. It has been suggested that T_K represents the temperature region below which the translational molecular motions responsible for the majority of unwanted physical and chemical changes in pharmaceutical products can be considered negligible over the normal product lifetime. Thus, T_K may indicate a conservative maximum storage temperature for amorphous pharmaceutical formulations, and may be considered a critical molecular mobility region for such systems [46].

To estimate T_K from simple calorimetric measurements, the equation proposed by Hancock et al. [46] was used (Eq. 4), assuming that the heat capacities of the liquid (C_{pl}) and crystalline states (C_{pc}) are approximately equal:

$$T_K = T_m - \left(\frac{\Delta H_m}{\Delta C_p}\right), \quad (4)$$

where T_m is the melting temperature, ΔH_m the heat of fusion, and ΔC_p is the heat capacity change at the T_g. T_Ks, indicated in Table 1, are 122.67 and 132.89 K, respectively, for NIC and CAB.

To confirm the appropriateness to approximate ΔC_p, the heat capacities of the liquid and crystalline states (respectively C_{pl} and C_{pc}) were measured by SS-DSC and then, according to Hancock et al. [46], the T_K was determined by Eq. 5:

$$T_K = T_m - \left(\Delta H_m / \left(C_{pl} - C_{pc}\right)\right). \quad (5)$$

The results are indicated in Table 1: in this case, the T_Ks were 136.01 and 147.64 K, respectively, for NIC and CAB. Comparison of these new results with those previously determined from Eq. 4 shows the similarity of the results

and thus the appropriateness of Eq. 4 for determining the T_K of the two drugs.

Conclusions

This study proved that it was possible to obtain NIC and CAB in their amorphous state by using different methods. In particular, the *Method C* may be considered the most appropriate for a possible industrial development of the amorphous form of NIC and CAB as active ingredient because more easily scalable. Experiments carried out by DSC proved the high stability of the amorphous form of the two drugs, NIC and CAB. For both substances, the relaxation time constants ranged from a few hours to many years, according to the aging temperatures, indicating the good thermodynamic stability of NIC and CAB in their glassy state. Experiments proved that even at a relatively low temperature used for the experiments (276 K), the stability of these drugs in their amorphous state is strongly increased and it is not necessary to reach the T_K to improve guarantee their stability. A temperature of 276 K is easily useful for industrial purposes and even the use of cold temperatures such as those of the fridge (approximately 288 K), frequently used in pharmacy to store some drug products, may be easily achieved, further improving the stability of these drugs. These results should encourage the development of solid dosage forms including these two drugs in their amorphous state, with no variations in physical state during the normal drug product shelf life. Further studies will be carried out to determine the physicochemical stability of NIC and CAB in their amorphous state, by evaluating the effect of water and in the presence of excipients. In addition, the biopharmaceutical properties (solubility, dissolution rate) of the amorphous forms will be evaluated compared to the crystalline ones.

References

1. Yu L. Amorphous pharmaceutical solids: preparation, characterization and stabilization. Adv Drug Deliv Rev. 2001;48:27–42.
2. Hancock BC. Disordered drug delivery: destiny, dynamics and the Deborah number. J Pharm Pharmacol. 2002;54:737–46.
3. Chawla G, Bansal AK. A comparative assessment of solubility advantage from glassy and crystalline forms of a water-insoluble drug. Eur J Pharm Sci. 2007;32:45–57.
4. Leuner C, Dressman J. Improving drug solubility for oral delivery using solid dispersions. Eur J Pharm Biopharm. 2000;50:47–60.
5. Ambike AA, Mahadik KR, Paradkar A. Stability study of amorphous valdecoxib. Int J Pharm. 2004;282:151–62.
6. Watanabe T, Wakiyama N, Usui F, Ikeda M, Isobe T, Senna M. Stability of amorphous indomethacin compounded with silica. Int J Pharm. 2001;226:81–91.
7. Shimpi SL, Chauhan B, Mahadik KR, Paradkar A. Stabilization and improved in vivo performance of amorphous etoricoxib using gelucire 50/13. Pharm Res. 2005;22:1727–34.
8. Gashi Z, Censi R, Malaj L, Gobetto R, Mozzicafreddo M, Angeletti M, Masic A, Di Martino P. Differences in the interaction between arylpropionic acid derivatives and poly(vinylpyrrolidone) K30: a multi-methodological approach. J Pharm Sci. 2009;98:4216–28.
9. Heitz C, Descombes JJ, Miller RC, Stoclet JC. α-adrenoceptor antagonistic and calcium antagonistic effects of nicergoline in the rat isolated aorta. Eur J Pharmacol. 1986;123:279–85.
10. Brossi A. The alkaloids. Chemistry and pharmacology, vol 38. San Diego: Academic Press Inc; 1990. p. 142.
11. Venn RD. Review of clinical studies with ergots in gerontology. In: Goldstein M, Liberman A, Calne DB, Thorner MO, editors. Ergot compounds and brain function. New York: Raven Press; 1980. p. 363–77.
12. Goo D, Palosi E, Szporny L. Comparison of the effects of vinpocetine, vincamine, and nicergoline on the normal and hypoxia-damaged learning process in spontaneously hypertensive rats. Drug Dev Res. 1988;15:75–85.
13. Pastoris O, Vercesi L, Allorio F, Dossena M. Effect of hypoxia, aging and pharmacological treatment on muscular metabolites and enzyme activities. Il Farmaco Ed Sci. 1988;43:627–42.
14. Triulzi E, Devizzi S, Margonato A. Use of nicergoline in acute myocardial infarction with diastolic hypertension. Il Farmaco Ed Prat. 1981;36:449–55.
15. Hušák M, Had J, Kratochvíl B, Cvak L, Stuchlík J, Jegorov A. X-ray absolute structure of nicergoline (form I). Quantitative analysis of nicergoline phase mixture: FormI/form II. Collect Czechoslov Chem Commun. 1994;59:1624–36.
16. Hušák M, Kratochvil B, Ondraček J, Maixner J, Jerolov A, Stuchlik J. The crystal and absolute molecular structure of "low melting" nicergoline (form II). Z Kristallogr. 1994;209:260–2.
17. Foresti E, Sabatino P, Riva di Sanseverino L, Fusco R, Tosi C, Tonani R. Structure and molecular orbital study of ergoline derivatives. 1-(6-Methyl-8β-ergolinylmethyl)imidazolidine-2,4-dione (I) and 2-(10-methoxy-1,6-dimethyl-8β-ergolinyl)ethyl 3,5-dimethyl-1H-2-pyrrolecarboxylate toluene hemisolvate (II) and comparison with nicergoline (III). Acta Cryst. 1988;B44:307–15.
18. Malaj L, Censi R, Capsoni D, Pellegrino L, Bini M, Ferrari S, Gobetto R, Massarotti V, Di Martino P. Characterization of nicergoline polymorphs crystallized in several organic solvents. J Pharm Sci. 2011;100:2610–22.
19. Colao A, Di Sarno A, Pivonello R, Di Somma C, Lombardi G. Dopamine receptor agonists for treating prolactinomas. Expert Opin Investig Drugs. 2002;11:787–800.
20. Olanow CW. The scientific basis for the current treatment of Parkinson's disease. Ann Rev Med. 2004;55:41–60.
21. Sabatino P, Riva Di Sanseverino L, Tonani R. X-ray crystal structure and conformational analysis of *N*-(3-dimethylaminopropyl)-*N*-(ethylaminocarbonyl)-6-(2-propenyl)ergoline-8β-carboxamide (cabergoline): comparison with bromocriptine and lisuride and a hypothesis for its high dopaminergic activity. Il Farmaco. 1995;50:175–8.
22. Bednář R, Cvak L, Čejka J, Kratochvíl B, Císařová I, Jegorov A. Cabergoline, form VII. Acta Cryst. 2004;E60:o1167–9.
23. Jegorov A, Cvak L, Bednář R, Čejka J, Hušák M, Kratochvíl B, Císařová I. Structures of cabergoline anhydrate form II and novel cabergoline solvates. Struct Chem. 2006;17:131–7.
24. Hanckock BC, Zografi G. Characteristics and significance of the amorphous state. J Pharm Sci. 1997;6:1–12.
25. Di Martino P, Palmieri GF, Martelli S. Molecular mobility of the paracetamol amorphous form. Chem Pharm Bull. 2000;48:1105–8.

26. Cao J, Long Y, Shanks RA. Experimental investigation into the heat capacity measurement using an modulated DSC. J Therm Anal Calorim. 1997;50:365–73.
27. Venkata Krishnan R, Nagarajan K. Evaluation of heat capacity measurements by temperature-modulated differential scanning calorimetry. J Therm Anal Calorim. 2010;102:1135–40.
28. Zografi G. States of water associated with solids. Drug Dev Ind Pharm. 1988;14:1905–26.
29. Ahlneck C, Zografi G. The molecular basis of moisture effects on the physical and chemical stability of drugs in the solid state. Int J Pharm. 1990;62:87–95.
30. Andronis V, Yoshioka M, Zografi G. Effect of sorbed water on crystallization of indomethacin from the amorphous state. J Pharm Sci. 1997;86:346–51.
31. Schmitt E, Davis CW, Long ST. Moisture-dependent crystallization of amorphous lamotrigine mesylate. J Pharm Sci. 1996;85:1215–9.
32. Tong P, Zografi G. Solid-state characteristics of amorphous indomethacin relative to its free acid. Pharm Res. 1999;16:1186–92.
33. Gunawan L, Johari GP, Shanker RM. Structural relaxation of acetaminophen glass. Pharm Res. 2006;23:967–79.
34. Di Martino P. Crystal growth from pharmaceutical melts. In: Seifer ED, editor. Bosons, ferromagnetism and crystal growth research. Horizons in world physics, vol. 257. New York: Nova Publisher; 2007. p. 221–45.
35. Van den Mooter G, Augustijns P, Kinget R. Stability prediction of amorphous benzodiazepines by calculation of the mean relaxation time constant using the Williams-Watts decay function. Eur J Pharm Biopharm. 1999;48:43–8.
36. Six K, Verreck G, Peeters J, Augustijns P, Kinget R, Van den Mooter G. Characterization of glassy itraconazole: a comparative study of its molecular mobility below T_g with that of structural analogues using MTDSC. Int J Pharm. 2001;213:163–73.
37. Vasukumar K, Bansal AK. Enthalpy relaxation studies on celecoxib amorphous mixtures. Pharm Res. 2002;19:1873–8.
38. Marsac PJ, Konno H, Taylor LS. A comparison of the physical stability of amorphous felodipine and nifedipine systems. Pharm Res. 2006;23:2306–16.
39. Montserrat S. Physical aging studies in epoxy resins. I. Kinetics of the enthalpy relaxation process in a fully cured epoxy resin. J Polym Sci B Polym Phys. 1994;32:509–22.
40. Fukuoka E, Makita M, Yamamura S. Glassy state of pharmaceuticals. III. Thermal properties and stability of glassy pharmaceuticals and their binary glass systems. Chem Pharm Bull. 1989;37:1047–50.
41. Yoshioka M, Hancock BC, Zografi G. Crystallization of indomethacin from the amorphous state below and above its glass transition temperature. J Pharm Sci. 1994;83:1700–5.
42. Hancock BC, Shamblin SL, Zografi G. Molecular mobility of amorphous pharmaceutical solids below their glass transition temperatures. Pharm Res. 1995;12:799–806.
43. Bauwens-Crowet C, Bauwens JC. Annealing of polycarbonate below the glass transition temperature. Polymer. 1986;27:709–13.
44. Kemmish DJ, Hay JN. The effect of physical ageing on the properties of amorphous PEEK. Polymer. 1985;26:905–12.
45. Williams G, Watts DC. Non-symmetrical dielectric relaxation behaviour arising from a simple empirical decay function. Trans Faraday Soc. 1970;66:80–5.
46. Hancock BC, Christensen K, Shamblin SL. Estimating the critical molecular mobility temperature (T_K) of amorphous pharmaceuticals. Pharm Res. 1998;15:1649–50.